Effect of particle asphericity on single-scattering parameters: comparison between Platonic solids and spheres

Ping Yang, George W. Kattawar, and Warren J. Wiscombe

The single-scattering properties of the Platonic shapes, namely, the tetrahedron, hexahedron, octahedron, dodecahedron, and icosahedron, are investigated by use of the finite-difference time-domain method. These Platonic shapes have different extents of asphericity in terms of the ratios of their volumes (or surface areas) to those of their circumscribed spheres. We present the errors associated with four types of spherical equivalence that are defined on the basis of (a) the particle's geometric dimension (b) equal surface area (A), (c) equal volume (V), and (d) equal-volume-to-surface-area ratio (V/A). Numerical results show that the derivations of the scattering properties of a nonspherical particle from its spherical counterpart depend on the definition of spherical equivalence. For instance, when the Platonic and spherical particles have the same geometric dimension, the phase function for a dodecahedron is more similar than that for an icosahedron to the spherical result even though an icosahedron has more faces than a dodecahedron. However, when the nonspherical and spherical particles have the same volume, the phase function of the icosahedral particle essentially converges to the phase function of the sphere, whereas the result for the dodecahedron is quite different from its spherical counterpart. Furthermore, the present scattering calculation shows that the approximation of a Platonic solid with a sphere based on V/A leads to larger errors than the spherical equivalence based on either volume or projected area.

OCIS codes: 010.1110, 010.1310, 290.1090, 290.1310, 290.2200, 290.5850.

1. Introduction

The scattering and absorption properties of nonspherical particles are fundamentally important to a number of science disciplines and many industrial applications. The importance of this subject can be recognized from the fact that substantial research efforts from the electromagnetic and optical research communities have been focused on developing various accurate and approximate methods to tackle the difficulty associated with the electromagnetic scattering by nonspherical particles. These methods were recently reviewed by Wriedt,[1] Mishchenko *et al.*,[2] Kahnert,[3] and Liou.[4] With these scattering computational methods, the optical characteristics of various nonspherical particles ranging from various axisymmetric geometries to highly irregular and inhomogeneous particle morphologies have been investigated. For example, Mugnai and Wiscombe,[5] Wiscombe and Mugnai,[6] Barber and Hill,[7] Mishchenko *et al.*,[8] and Schulz *et al.*[9] have investigated the optical properties of axially rotational particles (e.g., Chebyshev particles, spheroids, and finite-length circular cylinders); Fuller,[10] Mackowski,[11] and Mackowski and Mishchenko[12] have investigated the optical properties of spherical clusters; and many others (e.g., Liou *et al.*,[13] Videen *et al.*,[14] Sun *et al.*,[15] and Wriedt[16]) have investigated the optical properties associated with numerous types of particle morphology.

For electromagnetic scattering by a dielectric particle, the particle shape, in addition to the particle inherent dielectric characteristics (e.g., permittivity), largely affects the scattering properties of the particle. According to Barett,[17] particle shape, a synonym for particle geometric form in the literature, is the expression of particle external morphology. Specifically, particle shape can be qualitatively described by use of three morphological features: over-

P. Yang (pyang@ariel.met.tamu.edu) and G. W. Kattawar are, respectively, with the Department of Atmospheric Sciences and the Department of Physics, Texas A&M University, College Station, Texas 77843. W. J. Wiscombe is with Code 913, NASA Goddard Space Flight Center, Greenbelt, Maryland 20771.

Received 28 November 2003; revised manuscript received 11 May 2004; accepted 17 May 2004.

0003-6935/04/224427-09$15.00/0

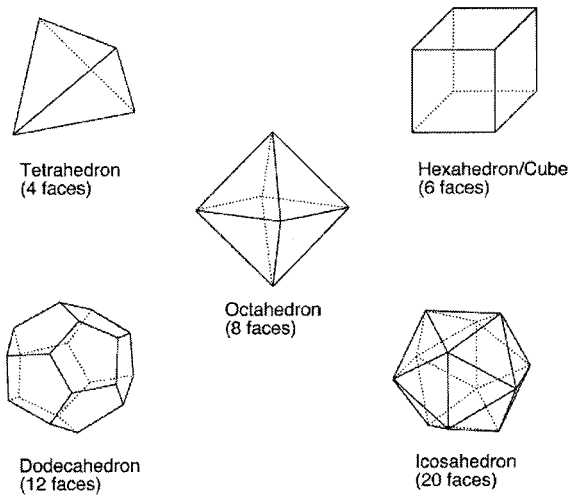

Fig. 1. Geometries of five Platonic shapes that include the tetrahedron, cube, octahedron, dodecahedron, and icosahedron.

all shape, roundness (or smoothness) of corners or edges, and surface texture. Additionally, the extent of particle convexity may also be an important morphological parameter. It has been shown that the optical properties of particles with smooth and sharp-edged surfaces (e.g., spheroids and finite circular cylinders)[18] are sensibly different. The extent of asphericity on the overall shape of a nonspherical particle is usually measured quantitatively in terms of the ratio of the volume (or surface area) of the particle to that of its circumscribed sphere.

Many nonspherical particles in nature have aspect ratios (note that the aspect ratio of a particle is defined as the ratio of its length to width) that are approximately equal to unity. This category of nonspherical particles, usually referred to as quasi-spherical particles, is often used in various practical applications involving the single-scattering properties of small particles. For example, they are important for a correct representation of the effect of small ice crystals on the radiative properties of ice clouds in a parameterization scheme, as shown by McFarquhar *et al.*[19] Note that the scattering properties of the quasi-spherical particles can be quite different from those of perfect spheres (e.g., Refs. 20 and 21).

The intent of the present study is to understand the effect of the asphericity on the scattering characteristics of the particles that possess sharp edges and planar faces. Specifically, we investigate a family of convex shapes known as Platonic solids consisting of the tetrahedron, cube, octahedron, dodecahedron, and icosahedron, all of which have different extents of asphericity specified in terms of the ratios of the particle volumes to those of the spheres that may be circumscribed around or inscribed within the particles. These Platonic particle shapes all have an aspect ratio of unity defined with respect to their circumscribed spheres, and they approach a sphere in an ordered manner. Thus the Platonic shapes are quite ideal for studying the general features regarding the asphericity effect on scattering properties. In the present study the finite-difference time-domain (FDTD) method pioneered by Yee[22] is used to calculate the single-scattering parameters of the Platonic particles. This paper is organized as follows. The geometrical shapes of the Platonic solids are described in Section 2. In Section 3 we briefly outline the method used for the present light-scattering calculation. The optical properties of the Platonic solids as compared with those of spheres are also discussed in Section 3. Finally, the conclusions of this study are given in Section 4.

2. Geometric Shapes of Platonic Solids

To study the effect of particle morphology on particle optical properties, we consider several polyhedral geometries for light-scattering calculations. Specifically, we consider the well-known Platonic solids (also known as regular polyhedrons), which usually means five geometric shapes: the tetrahedron, cube (or hexahedron), octahedron, dodecahedron, and icosahedron.[23–26] Figure 1 shows the geometries of the five Platonic solids. The numbers of the faces for the tetrahedron, cube, octahedron, dodecahedron, and icosahedron are 4, 6, 8, 12, and 20, respectively. The faces of a Platonic solid are equilateral polygons with the same number of sides. Note that the number of faces, the number of vertices, and the number of edges of a polyhedron satisfy the famous Euler's theorem.[27]

The five Platonic solids have quite different extents of asphericity measured quantitatively in terms of the ratios of either surface areas or volumes of these nonspherical geometries to those of their circumscribed spheres. Table 1 lists the ratios of the edge lengths (L) of the nonspherical Platonic solids to the corresponding circumscribed spherical radii (R), the

Table 1. Relationships for the Geometric Parameters for Platonic Particles[a]

Type	Number of Faces	L/R	r/R	$A/(4\pi R^2)$	$V/(4\pi R^3/3)$
Tetrahedron	4	1.63	0.33	0.37	0.12
Cube	6	1.15	0.58	0.64	0.37
Octahedron	8	1.41	0.58	0.55	0.32
Dodecahedron	12	0.71	0.79	0.84	0.66
Icosahedron	20	1.05	0.79	0.76	0.61

[a]L is the edge length of a Platonic particle, R is the radius of the circumscribed sphere, r is the radius of the inscribed sphere, A is the surface area, and V is the volume of a Platonic particle.

ratios of the radii of the corresponding inscribed spheres (r) to those of the circumscribed spheres, the ratios of the surface areas (A) of the Platonic solids to those of the circumscribed spheres, and the ratios of the volumes (V) of the Platonic solids to those of the circumscribed spheres. From the surface area ratios or volume ratios listed in Table 1, it is evident that the tetrahedral shape among the five Platonic solids has the maximum asphericity, whereas the dodecahedral shape has the minimum asphericity.

To understand the scattering characteristics of the Platonic solids when compared with their spherical counterparts, we consider four types of spherical equivalence for the nonspherical particles. First, we define the circumscribed sphere of a Platonic particle as its spherical equivalence; i.e., the nonspherical and spherical particles have the same geometric dimension. Second, we define an equivalent-surface sphere whose radius is given by

$$R_a = (A/4\pi)^{1/2}, \tag{1}$$

where A is the surface area of a Platonic particle. Additionally, we also define the volume-equivalent sphere whose radius is given by

$$R_v = (3V/4\pi)^{1/3}, \tag{2}$$

where V is the volume of a Platonic particle. Following Foot,[28] Francis *et al.*,[29] Mitchell and Arnott,[30] Wyser and Yang,[31] Fu *et al.*,[32] and Grenfell and Warren,[33] we also define the effective spherical radius for a nonspherical particle as follows:

$$R_{\text{eff}} = \frac{3}{4}\frac{V}{A_p}, \tag{3a}$$

where A_p is the averaged particle projected area. For an arbitrary convex particle, it has been proven[34] that A_p equals $A/4$ under random orientations. Thus, the effective radius defined in Eq. (3a) is the same as the following definition:

$$R_{\text{eff}} = 3V/A \tag{3b}$$

Note that the ratio of the volume to the projected area is proportional to the mean length of the particles in the anomalous diffraction theory originally developed by van de Hulst.[35] Because the anomalous diffraction theory can give some physical insight into processes associated with light scattering by a large dielectric particle when the refractive index is small, the spherical equivalence defined in terms of the effective radius in Eq. (3b) is expected to be more suitable than the volume- or surface-area-based equivalence. For this reason, the spherical equivalence based on Eq. (3a) has been advocated (e.g., Fu *et al.*[32]). Table 2 lists the ratios of the radii of circumscribed spheres to the equivalent radii defined in Eqs. (1)–(3) for the five Platonic shapes. Evidently, among the three definitions based on Eqs. (1)–(3a) for spherical equivalence, the surface-area-based-equivalent spherical radius (R_a) is the largest, whereas the effective radius (R_{eff}) is the smallest.

Table 2. Ratios of R to R_a, R_v, and R_{eff}[a]

Type	R/R_a	R/R_v	R/R_{eff}
Tetrahedron	1.65	2.01	3.00
Cube	1.25	1.40	1.73
Octahedron	1.35	1.46	1.73
Dodecahedron	1.09	1.15	1.26
Icosahedron	1.15	1.18	1.26

[a] R is the radius of the circumscribed sphere; R_a is the radius of the equivalent-surface-area sphere; R_v is the radius of the equivalent-volume sphere; and $R_{\text{eff}} = 3V/A$ in which V is the volume and A is the surface area of a given polyhedron.

The minimum of R/R_a (and also R/R_v) ratio values, which implies the maximum extent of sphericity for the nonspherical particles, is observed for the dodecahedral geometry. However, the dodecahedron and icosahedron have the same extent of asphericity if specified in terms of R/R_{eff} (note that R/R_{eff} is 1.26 for both geometries). The same feature is also noted for the cube and octahedron, i.e., $R/R_{\text{eff}} = 1.73$ for the two shapes. Thus the spherical equivalence based on V/A has a disadvantage in the sense that the extent of asphericity cannot be uniquely specified in some cases.

3. Scattering Properties of Platonic Particles

A number of methods have been developed for calculating the scattering properties of nonspherical particles, among which the T-matrix method,[16,36,37] the discrete dipole approximation,[38,39] and the FDTD[38,39] method[40–43] are the most widely used. In this study we use the FDTD method to compute the single-scattering properties of the Platonic particles. The FDTD method is flexible in dealing with an arbitrary nonspherical particle morphology in the sense that the representation of a scatterer in this method is straightforward, by assignment of proper permittivities over grid points. The basic principle of this method is to compute the near field via a finite-difference analog of two time-dependent Maxwell's curl equations given by

$$\nabla \times \mathbf{H} = \frac{\epsilon}{c}\frac{\partial \mathbf{E}}{\partial t}, \tag{4a}$$

$$\nabla \times \mathbf{E} = -\frac{\mu}{c}\frac{\partial \mathbf{H}}{\partial t}, \tag{4b}$$

where $\mathbf{E}$ and $\mathbf{H}$ are electric and magnetic fields, respectively, and ϵ and μ are permittivity and permeability, respectively. To implement the finite-difference computation, we use the perfectly matched layer boundary condition developed by Berenger[44] to truncate the spatial domain. The near field obtained in the time domain, which is directly computed from a finite-difference form of the time-dependent Maxwell equations, can be transformed into its far-field counterpart via the Fourier transform. Furthermore, the near field can be transformed into the far field via an exact electrodynamic relationship.

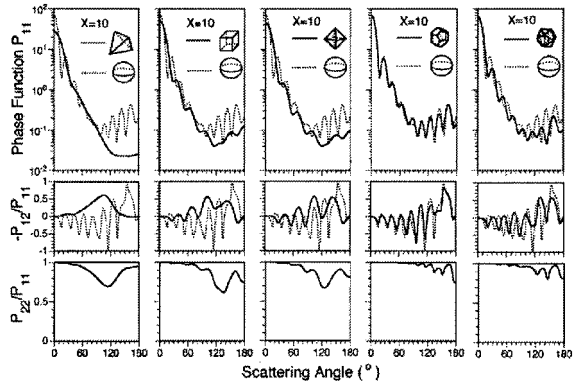

Fig. 2. Phase function, degree of linear polarization ($-P_{12}/P_{11}$), and P_{22}/P_{11} for the Platonic shapes and the corresponding circumscribed spheres (i.e., the spheres and the Platonic shapes have the same geometric dimension) at a wavelength of 0.6328 μm. The particles are assumed to be ice with a refractive index of $m = 1.3085 + i1.09 \times 10^{-8}$.

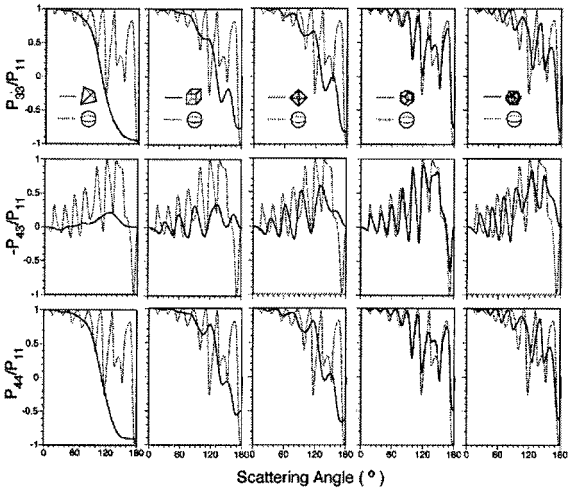

Fig. 3. Same as Fig. 2 except for P_{33}/P_{11}, $-P_{43}/P_{11}$, and P_{44}/P_{11}.

The details of the FDTD technique for an application to the light-scattering computation can be found in the literature (e.g., Refs. 40–43). The scattering phase matrix of a nonspherical particle depends on the orientation of the particle relative to the incident beam direction, the scattering angle, and the azimuthal angle of the scattering plane on which the scattered field is observed. For simplicity, we assume the Platonic particles are randomly orientated in space. Under this condition, the phase matrix is independent of the azimuthal angle of the scattering plane. In this study we define the phase matrix following Bohren and Huffman.[45]

Figure 2 shows the phase function P_{11}, the degree of linear polarization that is given by $-P_{12}/P_{11}$, and the ratio of P_{22}/P_{11} for the five Platonic shapes, which are compared with the results for the circumscribed spheres. The size parameter $x = 10$ in Fig. 2 is defined with respect to the radius of the circumscribed sphere, that is, $2\pi R/\lambda = 10$. The wavelength used in the scattering calculation is 0.6328 μm, and the refractive index is assumed to be that of ice at this wavelength, given by $m = 1.3085 + i1.09 \times 10^{-8}$ from the data compiled by Warren.[46] For the phase function, the spherical result displays pronounced oscillations, particularly, for scattering angles ranging from 120° to 180°. The phase function for the tetrahedral shape is quite featureless and essentially flat near backscattering directions. Unlike the phase function for the tetrahedron, the phase functions for the other four types of the Platonic shape also show some oscillations. The phase functions for the hexahedron and octahedron are quite similar, although the result for the former is closer to that of the sphere around the 60° scattering angle. The phase function for the dodecahedron is similar to that of the sphere because the dodecahedron among the five shapes has the maximum sphericity. The results for $-P_{12}/P_{11}$ also show that the results for nonspherical particles approach their spherical counterparts when the sphericity of the Plantonic particles increases in the order of the tetrahedron, hexahedron, octahedron, icosahedron, and dodecahedron. The quantity P_{22}/P_{11} is indicative of the asphericity of a particle[45,47] because this parameter is unity for a sphere. Evidently, the results for the five Platonic shapes indicate the nonspherical effect. It is noteworthy that the values of P_{22}/P_{11} for the dodecahedron and icosahedron are of the same order, although the phase function and $-P_{12}/P_{11}$ for the former are much closer to their spherical counterparts. The quantity $(1 - P_{22}/P_{11})$ is sometimes called the depolarization ratio.[45] From the comparison between the nonspherical and the spherical results shown in Fig. 2, it is evident that the depolarization ratio is more sensitive than the degree of linear polarization to the particle nonsphericity. Especially, the values of P_{22}/P_{11} at large scattering angles are quite sensible to particle nonsphericity. Furthermore, the extent of asphericity for the five Platonic particles can be ranked in the order of the tetrahedron, octahedron, hexahedron, icosahedron, and dodecahedron. This is consistent with the asphericity rank illustrated by the numbers listed in Table 1. To illustrate this point even further, we show the other elements of the phase matrix in Fig. 3, namely, P_{33}/P_{11}, $-P_{43}/P_{11}$, and P_{44}/P_{11}. We see here that, even for the dodecahedron whose phase function agrees well with that of the sphere, there are large differences when these other elements are compared. It should be noted that these phase-matrix elements are sensitive to the phase of the fields and not just their moduli.

Figure 4 shows the phase function of an ice sphere with a size parameter of $x = 5$ at a wavelength of 0.6328 μm. Also shown in Fig. 4 are the phase functions of the five Platonic shapes with the same radius, projected area, volume, and V/A (the first, second, third, and fourth columns, respectively, in Fig. 4) as those for the sphere. Because the orientation-averaged projected area of a convex shape is one fourth of the particle surface area under the random

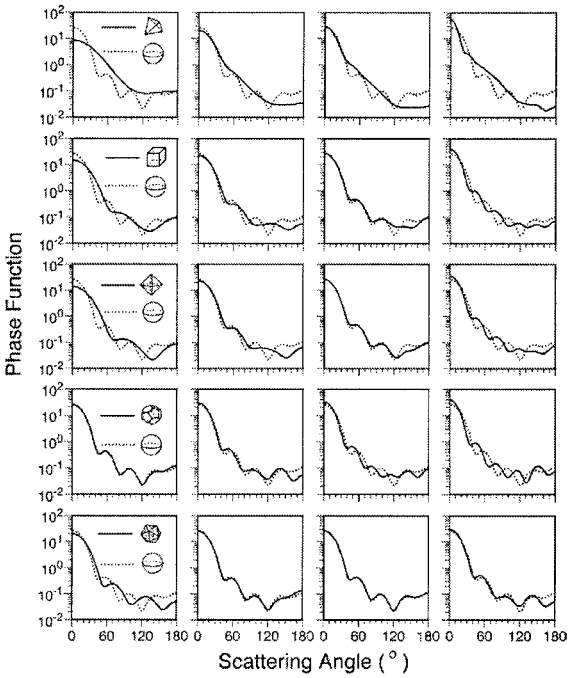

Fig. 4. Phase function of an ice sphere with a size parameter of $x = 5$. The wavelength and refractive index are the same as those in Fig. 2. Also shown are the phase functions of the five Platonic shapes with the same radius (the first column), projected area (the second column), volume (the third column), and V/A (the fourth column) as those for the sphere.

orientation condition, the projected-area-based equivalence is the same as the surface-area-based equivalence. The four types of nonspherical–spherical equivalence in Fig. 4 are hereafter referred to as R-based equivalence, A-based equivalence, V-based equivalence, and V/A-based equivalence (the first, second, third, and fourth columns, respectively, in Fig. 4). The results shown in the first column of Fig. 4 indicate that the forward-scattering peaks for the tetrahedron, hexahedron, and octahedron are substantially lower than those for the sphere. Because the forward-scattered peak is due primarily to diffraction, we should expect the largest deviation to occur for those particles whose projected area deviates the greatest amount from their spherical counterparts. This is especially noticeable in the case of the tetrahedron because a tetrahedron has a much smaller projected area than its circumscribed sphere does. When the dimensions of the nonspherical particles and the sphere are the same, the phase function for the dodecahedron is quite similar to that for the sphere. This is because the dodecahedron, among the five Platonic shapes, has the minimum deviation from asphericity. The phase functions for the other four Platonic shapes are quite different from those associated with their circumscribed spheres. The second and third columns in Fig. 4 correspond to the cases for the surface-area-based and volume-based equivalences, respectively. When the surface area or volume of the nonspherical particles are defined to be the same as that of the sphere, the forward-scattering peaks of the phase functions for the Platonic shapes are quite similar to their spherical counterparts. An interesting feature to note is that the icosahedron has the minimum extent of asphericity for the light-scattering computation if the nonspherical and spherical particles have the same volume or surface area. The phase function for the icosahedron essentially converges to the spherical result when the volumes for the two geometric shapes are equal. This feature well illustrates the importance of how a spherical equivalence is defined. The fourth column in Fig. 4 is the case in which the Platonic particles and the sphere have the same V/A. Evidently, the spherical equivalence based on the V/A is less accurate than either the surface-area-based or the volume-based spherical equivalence. Although the V/A-based spherical approximation has been advocated in practice, Fig. 4 shows that the volume-based spherical equivalence is the most suitable in the case of small size parameters. It should be pointed out that the present V/A-based spherical equivalence is different from that suggested by Grenfell and Warren.[33] By use of Eq. (3a) or (3b), in this study a nonspherical particle is approximated by a single sphere. In contrast, in Grenfell and Warren's approach, a population of polydisperse nonspherical particles is involved, and an individual nonspherical particle is replaced by a number of spheres. The spherical equivalence suggested by Grenfell and Warren[33] provides an effective alternative to deal with particle asphericity in the light-scattering computation as applied to atmospheric radiative transfer simulation, particularly, flux computation.

Figure 5 is the same as Fig. 4, except for a wavelength of 11 μm. The refractive index of ice at this wavelength is $1.0925 + i0.248$. It should be noted that ice is strongly absorptive at this wavelength because the imaginary part of the refractive index is quite large. Additionally, the 11-μm wavelength for ice is within the Christiansen band[48,49] in which the extinction of an ice particle is minimum because the real part of the refractive index is close to 1. The overall features shown in Fig. 5 are similar to those in Fig. 4; namely, the dodecahedral particle has the minimum extent of asphericity if the Platonic particles and the sphere have the same dimension, whereas the minimum nonspherical effect is noted for the icosahedron if the volume or surface area is conserved. In the case involving strong absorption, an interesting point to note is that the radius-based spherical equivalence overestimates the forward-scattering peak of the phase function, whereas the scattering peak in the forward direction is underestimated in the spherical equivalence based on V/A, as is evident from results shown in the first and fourth columns in Fig. 5.

In that many aerosols have a higher refractive index (both real and imaginary parts) than ice at a visible wavelength, we performed a calculation similar to the results presented in Fig. 4 except the refractive index was taken as $m = 1.53 + i8 \times 10^{-3}$ (see Mishchenko *et al.*[50]) for a wavelength of 0.55 μm; the

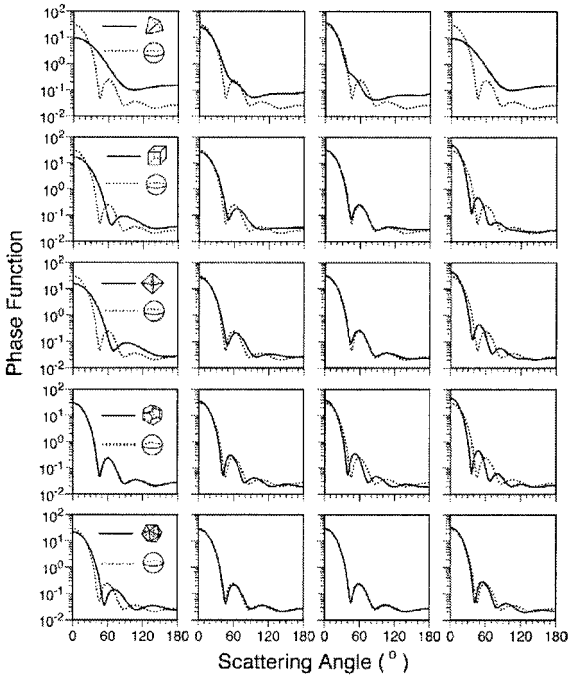

Fig. 5. Same as Fig. 4 except for a wavelength of 11 μm. The refractive index of ice at this wavelength is $1.0925 + i0.248$.

size parameter was kept the same, namely, $x = 5$. The results are shown in Fig. 6, and, if one compares these results with those for ice shown in Fig. 4, one can see that they are in complete qualitative agreement with them.

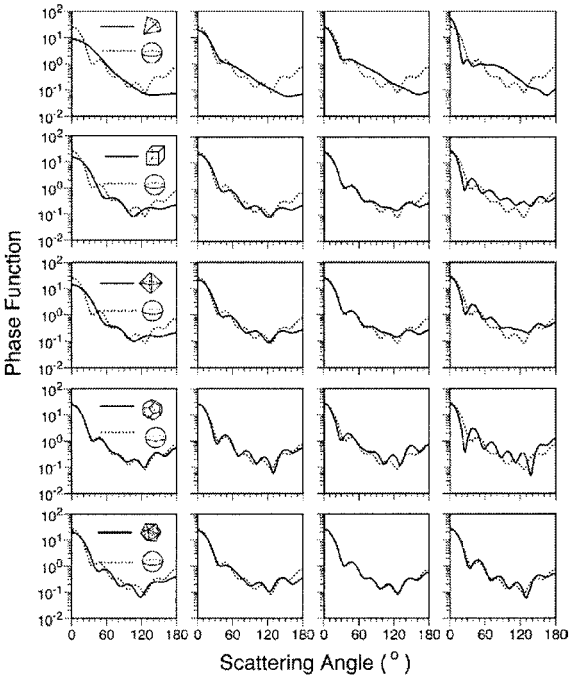

Fig. 6. Same as Fig. 4 except the particles are assumed to be aerosols with a refractive index $m = 1.53 + i8 \times 10^{-3}$ for a wavelength of 0.55 μm; the size parameter was kept the same, namely, $x = 5$.

Table 3 lists the extinction efficiencies and single-scattering albedos associated with the phase functions shown in Figs. 4 and 5. Evidently, the extinction efficiencies (i.e., the ratio of the extinction cross section to the particle projected area) and single-scattering albedos for spheres and the Platonic shapes are different, depending on a specific spherical equivalence. In Figs. 4 and 5 it is shown that the dodecahedron and the spheres have similar phase functions if the dimensions of these two types of particle are the same. However, according to the numbers listed in Table 3, the relative differences of the extinction efficiencies of the dodecahedral and spherical particles are 12.5% and 14.8% at 0.6328- and 11-μm wavelengths, respectively. Note that the projected areas of the Platonic solids are smaller than those of their circumscribed spheres. If the differences of the projected areas are accounted for, the difference of the extinction cross sections of a Platonic and a sphere is given by

$$\text{Difference} = \frac{[Q_{\text{ext, Platonic}} A/(4\pi R^2) - Q_{\text{ext,sphere}}]}{Q_{\text{ext,sphere}}}, \quad (5)$$

where $Q_{\text{ext,Platonic}}$ and $Q_{\text{ext,sphere}}$ are the extinction efficiencies for the Platonic solids and spheres, respectively. From Eq. (5) and the area ratio given in Table 1, the preceding two relative errors (12.5% and 14.8%) reduce to −5.8% and −3.9% for the differences between the extinction cross sections of the dodecahedrons and the corresponding circumscribed spheres. Similarly, in the case for the icosahedrons that have the same volumes as spheres, the relative differences for the extinction efficiencies are −8.2% and −6.6% for the cases listed in Table 3 for 0.6328- and 11-μm wavelengths, respectively. However, the corresponding relative differences for the extinction cross sections are −5.2% and −3.6%. Therefore it can be misleading to compare the extinction (or scattering) efficiencies instead of the extinction (or scattering) cross sections for nonspherical and spherical particles. An important point to note is that what is used in radiative transfer calculations is the extinction and scattering cross sections rather than efficiencies.

4. Conclusions

To understand the asphericity effect of nonspherical particles on their optical properties, we have computed the single-scattering parameters including the phase matrix, extinction efficiency, and single-scattering albedo for the well-known Platonic geometries for cases involving both negligible and strong absorptions. The size parameters involved in this study are in the resonant region that excludes the applicability of the commonly used geometric-optics method. Thus we use the FDTD method for the present light-scattering computations. The optical properties of these nonspherical particles are compared with four types of spherical counterpart that are based on equivalent geometric dimension, volume (V), surface area (A), and V/A. Numerical results

Table 3. Extinction Efficiencies and Single-Scattering Albedos Associated with the Phase Functions Shown in Figs. 4 and 5

		$\lambda = 0.6328\ \mu m$		$\lambda = 11\ \mu m$	
Shape	Equivalence	Extinction Efficiency	Single-Scattering Albedo	Extinction Efficiency	Single-Scattering Albedo
Sphere		3.36×10^{0}	1.00×10^{0}	1.82×10^{0}	3.78×10^{-1}
Tetrahedron	R-based equivalence	5.73×10^{-1}	1.00×10^{0}	8.74×10^{-1}	2.36×10^{-1}
	A-based equivalence	1.59×10^{0}	1.00×10^{0}	1.21×10^{0}	3.02×10^{-1}
	V-based equivalence	2.04×10^{0}	1.00×10^{0}	1.28×10^{0}	3.53×10^{-1}
	V/A-based equivalence	2.35×10^{0}	1.00×10^{0}	1.47×10^{0}	4.00×10^{-1}
Hexahedron	R-based equivalence	1.62×10^{0}	1.00×10^{0}	1.29×10^{0}	3.12×10^{-1}
	A-based equivalence	2.29×10^{0}	1.00×10^{0}	1.41×10^{0}	3.63×10^{-1}
	V-based equivalence	2.54×10^{0}	1.00×10^{0}	1.51×10^{0}	3.63×10^{-1}
	V/A-based equivalence	2.98×10^{0}	1.00×10^{0}	1.59×10^{0}	4.08×10^{-1}
Octahedron	R-based equivalence	1.56×10^{0}	1.00×10^{0}	1.31×10^{0}	3.02×10^{-1}
	A-based equivalence	2.44×10^{0}	1.00×10^{0}	1.49×10^{0}	3.57×10^{-1}
	V-based equivalence	2.68×10^{0}	1.00×10^{0}	1.54×10^{0}	3.71×10^{-1}
	V/A-based equivalence	3.02×10^{0}	1.00×10^{0}	1.62×10^{0}	3.96×10^{-1}
Dodecahedron	R-based equivalence	3.78×10^{0}	1.00×10^{0}	2.09×10^{0}	3.77×10^{-1}
	A-based equivalence	4.03×10^{0}	1.00×10^{0}	2.16×10^{0}	3.91×10^{-1}
	V-based equivalence	4.22×10^{0}	1.00×10^{0}	2.18×10^{0}	3.98×10^{-1}
	V/A-based equivalence	4.35×10^{0}	1.00×10^{0}	2.23×10^{0}	4.12×10^{-1}
Icosahedron	R-based equivalence	2.54×10^{0}	1.00×10^{0}	1.61×10^{0}	3.48×10^{-1}
	A-based equivalence	3.00×10^{0}	1.00×10^{0}	1.71×10^{0}	3.70×10^{-1}
	V-based equivalence	3.09×10^{0}	1.00×10^{0}	1.70×10^{0}	3.81×10^{-1}
	V/A-based equivalence	3.25×10^{0}	1.00×10^{0}	1.73×10^{0}	3.94×10^{-1}

show that all the spherical approximations lead to pronounced errors (particularly, at a visible wavelength) for the first three Platonic geometries (i.e., tetrahedron, hexahedron, and octahedron) due to the substantial extent of asphericity in these cases. Among the four spherical approximations, the spherical equivalence based on volume corresponds to minimum errors. The comparison of phase functions for the spherical and nonspherical particles is quite interesting in the cases of the dodecahedron and icosahedron. Although an icosahedron has more faces than a dodecahedron, the extent of asphericity for the former is more substantial than the case of the latter if the spherical equivalence is specified with respect to particle linear dimension (or diameter). In contrast, the reverse situation is true if the spherical equivalence is defined according to the volume of the Platonic particles. In other words, the extent of asphericity for a particle really depends on the definition of a specific spherical equivalence. The spherical approximation based on V/A (or projected area) does not lead to minimum errors, as compared with the other three types of spherical equivalence. Additionally, the spherical equivalence based on V/A cannot uniquely specify the extent of asphericity because this ratio is the same, both for a dodecahedron and an icosahedron if they have the same circumscribed diameter. In this study the spherical equivalence based on V/A is the approximation of a nonspherical particle with a single sphere. This V/A-based spherical approximation is different from that suggested by Grenfell and Warren who replaced a nonspherical particle by using a number of spheres in computing the optical properties of a population of polydisperse nonspherical particles. Grenfell and Warren's approach is a quite effective alternative in computing the bulk optical properties of a polydisperse system of nonspherical particles, as applied to the simulation of radiative transfer (flux computation, in particular) in the atmosphere. Furthermore, in this study we also show that it can be quite misleading to compare the extinction (or absorption) efficiencies rather than cross sections for a nonspherical particle and a spherical particle because they may have different cross sections projected on a plane normal to the incident direction. The present study is limited to small size parameters. It will be interesting to investigate these features associated with particle asphericity for size parameters in the regime of geometric optics.

This study is supported by a research grant from National Science Foundation (NSF) CAREER Award program (ATM-0239605 from NSF-Physical Meteorology Program managed by William A. Cooper) and by NASA research grants (NAG-1-02002 and NAG5-11374) from the NASA Radiation Sciences Program managed by Donald Anderson and Hal Maring. G. W. Kattawar's research is supported by the Office of Naval Research under contract N00014-02-1-0478.

References

1. T. Wriedt, "A review of elastic light scattering theories," Part. Part. Syst. Charact. **15,** 67–74 (1998).
2. M. I. Mishchenko, W. J. Wiscombe, J. W. Hovenier, and L. D. Travis, "Overview of scattering by nonspherical particles," in *Light Scattering by Nonspherical Particles: Theory, Measurements, and Applications,* M. I. Mishchenko, J. W. Hovenier, and L. D. Travis, eds. (Academic, San Diego, Calif., 2000), pp. 29–60.
3. F. M. Kahnert, "Numerical methods in electromagnetic scat-

tering theory," J. Quant. Spectrosc. Radiat. Transfer **79–80,** 775–824 (2003).
4. K. N. Liou, *An Introduction to Atmospheric Radiation,* 2nd ed. (Academic, San Diego, Calif., 2002).
5. A. Mugnai and W. J. Wiscombe, "Scattering from nonspherical Chebyshev particles. I: cross sections, single-scattering albedo, asymmetry factor, and backscattered fraction," Appl. Opt. **25,** 1235–1244 (1986).
6. W. J. Wiscombe and A. Mugnai, "Scattering from nonspherical Chebyshev particles. 2: Means of angular scattering patterns," Appl. Opt. **27,** 2405–2421 (1988).
7. P. W. Barber and S. C. Hill, *Light Scattering by Particles: Computational Methods* (World Scientific, Singapore, 1990).
8. M. I. Mishchenko, L. D. Travis, and D. W. Mackowski, "T-matrix computation of light scattering by nonspherical particles: a review," J. Quant. Spectrosc. Radiat. Transfer **55,** 535–575 (1996).
9. F. M. Schulz, K. Stamnes, and J. J. Stamnes, "Scattering of electromagnetic waves by spheroidal particles: a novel approach exploiting the T matrix computed in spheroidal coordinates," Appl. Opt. **37,** 7875–7896 (1998).
10. K. A. Fuller, "Optical resonances and two-sphere systems," Appl. Opt. **33,** 4716–4731 (1991).
11. D. W. Mackowski, "Calculation of total cross sections of multiple-sphere clusters," J. Opt. Soc. Am. A **11,** 2851–2861 (1994).
12. D. W. Mackowski and M. I. Mishchenko, "Calculation of the *T* matrix and the scattering matrix for ensembles of spheres," J. Opt. Soc. Am. A **13,** 2266–2278 (1996).
13. K. N. Liou, Y. Takano, and P. Yang, "Light scattering and radiative transfer in ice crystal clouds: applications to climate research," in *Light Scattering by Nonspherical Particles: Theory, Measurements, and Applications,* M. I. Mishchenko, J. W. Hovenier, and L. D. Travis, eds. (Academic, San Diego, Calif., 2000), pp. 417–1449.
14. G. Videen, W. Sun, and Q. Fu, "Light scattering from irregular tetrahedral aggregates," Opt. Commun. **156,** 5–9 (1998).
15. W. Sun, T. Nousiainen, K. Muinonen, Q. Fu, N. G. Loeb, and G. Videen, "Light scattering by Gaussian particles: a solution with finite-difference time-domain technique," J. Quant. Spectrosc. Radiat. Transfer **79–80,** 1083–1090 (2003).
16. T. Wriedt, "Using the T-matrix method for light scattering computations by non-axisymmetric particles: superellipsoids and realistically shaped particles," Part. Part. Syst. Charact. **4,** 256–268 (2002).
17. P. J. Barrett, "The shape of rock particles, a critical review," Sedimentology **27,** 291–303 (1980).
18. L. Liu and M. I. Mishchenko, "Constraints on PSC particle microphysics derived from lidar observations," J. Quant Spectrosc. Radiat. Transfer **70,** 817–831 (2001).
19. G. M. McFarquhar, P. Yang, A. Macke, and A. J. Baran, "A new parameterization of single-scattering solar radiative properties for tropical anvils using observed ice crystal size and shape distributions," J. Atmos. Sci. **59,** 2458–2478 (2002).
20. P. Yang, B. A. Baum, A. J. Heymsfield, Y. X. Hu, H.-L. Huang, S.-C. Tsay, and S. Ackerman, "Single-scattering properties of droxtals," J. Quant. Spectrosc. Radiat. Transfer **79–80,** 1159–1180 (2003).
21. T. Nousiainen and G. M. McFarquhar, "Light scattering by small quasi-spherical ice crystals: preliminary results," in *Proceedings of the 7th Conference on Electromagnetic and Light Scattering by Nonspherical Particles: Theory, Measurements, and Applications* (Universitäts-Buchhandlung, Bremen, Germany, 2003), pp. 271–274.
22. K. S. Yee, "Numerical solution of initial boundary problems involving Maxwell's equations in isotropic media," IEEE Trans. Antennas. Propag. **AP-14,** 302–307 (1966).
23. P. R. Cromwell, *Polyhedra* (Cambridge U. Press, Cambridge, UK, 1997).
24. L. A. Lyusternik, *Convex Figures and Polyhedra* (Heath, Boston, Mass., 1966).
25. B. Grunbaum, *Convex Polytopes* (Wiley, London, 1967).
26. M. J. Wenninger, *Polyhedron Models* (Cambridge U. Press, Cambridge, UK, 1970).
27. L. Euler, "Elementa Doctrinae Solidorum," Novi Commentarii Academiae Scientiarum Petropolitanae **4,** 109–140 (1758).
28. J. S. Foot, "Some observations of the optical properties of clouds. II: cirrus," Q. J. R. Meteorol. Soc. **114,** 145–164 (1988).
29. P. N. Francis, A. Jones, R. W. Saunders, K. P. Shine, A. Slingo, and Z. Sun, "An observational and theoretical study of the radiative properties of cirrus: some results from ICE'89," Q. J. R. Meteorol. Soc. **120,** 809–848 (1994).
30. D. L. Mitchell and W. P. Arnott, "A model predicting the evolution of ice particle size spectra and radiative properties of cirrus cloud. II. Dependence of absorption and extinction on ice crystal morphology," J. Atmos. Sci. **51,** 817–832 (1994).
31. K. Wyser and P. Yang, "Average crystal size and bulk shortwave single scattering properties in ice clouds," Atmos. Res. **49,** 315–335 (1998).
32. Q. Fu, W. Sun, and P. Yang, "On modeling of scattering and absorption by cirrus nonspherical ice particles at thermal infrared wavelengths," J. Atmos. Sci. **56,** 2937–2947 (1999).
33. T. C. Grenfell and S. G. Warren, "Representation of a nonspherical ice particle by a collection of independent spheres for scattering and absorption of radiation," J. Geophys. Res. **104,** 31697–31709 (1999).
34. V. Vouk, "Projected area of convex bodies," Nature (London) **162,** 330–331 (1948).
35. H. C. van de Hulst, *Light Scattering by Small Particles* (Wiley, New York, 1957).
36. M. I. Mishchenko, "Light scattering by randomly oriented axially symmetric particles," J. Opt. Soc. Am. A **8,** 871–882 (1991).
37. S. Havemann and A. J. Baran, "Extension of T-matrix to scattering of electromagnetic plane waves by non-axisymmetric particles: application to hexagonal ice cylinders," J. Quant. Spectrosc. Radiat. Transfer **70,** 139–158 (2001).
38. B. T. Draine, "The discrete-dipole approximation and its application to interstellar graphite grains," Astrophys. J. **333,** 848–872 (1988).
39. B. T. Draine and P. J. Flatau, "Discrete-dipole approximation for light calculations," J. Opt. Soc. Am. A **11,** 1491–1499 (1994).
40. A. Taflove, *Advances in Computational Electromagnetics* (Artech House, Boston, Mass., 1998).
41. P. Yang and K. N. Liou, "Finite-difference time domain method for light scattering by small ice crystals in three-dimensional space," J. Opt. Soc. Am. A **13,** 2072–2085 (1996).
42. P. Yang, K. N. Liou, M. I. Mishchenko, and B. C. Gao, "Efficient finite-difference time-domain scheme for light scattering by dielectric particles: application to aerosols," Appl. Opt. **39,** 3727–3737 (2000).
43. W. B. Sun, Q. Fu, and Z. Chen, "Finite-difference time-domain solution of light scattering by dielectric particles with a perfectly matched layer absorbing boundary condition," Appl. Opt. **38,** 3141–3151 (1999).
44. J. P. Berenger, "A perfect matched layer for the absorption of electromagnetic waves," J. Comput. Phys. **114,** 185–200 (1994).
45. C. F. Bohren and D. R. Huffman, *Absorption and Scattering of Light by Small Particles* (Wiley, New York, 1983).
46. S. G. Warren, "Optical constants of ice from the ultraviolet to the microwave," Appl. Opt. **23,** 1206–1225 (1984).

47. M. I. Mischenko, L. D. Travis, and A. A. Lacis, *Scattering, Absorption, and Emission of Light by Small Particles* (Cambridge U. Press, Cambridge, UK, 2002).
48. W. P. Arnott, Y. Y. Dong, and J. Hallett, "Extinction efficiency in the infrared (2–18 μm) of laboratory ice clouds: observations of scattering minima in the Christiansen bands of ice," Appl. Opt. **34,** 541–551 (1995).
49. P. Yang, K. N. Liou, and W. P. Arnott, "Extinction efficiency and single-scattering albedo of ice crystals in laboratory and natural cirrus clouds," J. Geophys. Res. **102,** 21825–21835 (1997).
50. M. I. Mishchenko, L. D. Travis, R. A. Kahn, and R. A. West, "Modeling phase functions for dustlike tropospheric aerosols using a shape mixture of randomly oriented polydisperse spheroids," J. Geophys. Res. **102,** 16831–16847 (1997).